Modeling of spontaneous phase separation in nanomaterials and confined systems with electron correlations

A. N. Kocharian [*], G. W. Fernando[**], Kun Fang[**], A. V. Balatsky[***]
[*]California State University, Los Angeles, CA 90032, USA
[**]University of Connecticut, Storrs, CT 06269, USA
[***]AlbaNova Univ. Center Nordita, SE-106 91, Stockholm, Sweden

ABSTRACT

The modeling of many body physics near possible spontaneous phase separation instabilities away from half filling in various square and honeycomb structures provide an ideal playground for understanding various competing phases in repulsive and attractive Hubbard models. Exact diagonalization, Lanczos and variational cluster approximation (VCA) techniques are critical for accurate studies of Rashba spin-orbit effects with short-range electron correlations to address current challenging problems in superconductivity, magnetism and topological insulators associated with numerous interfaces and heterostructures. The results highlight important aspects of interplay of the spin-orbit coupling with a magnetic field in graphene-like systems, tetrahedral pyrochlores, honeycomb sodium based iridates and unconventional superconductors induced by weak, moderate and strong electron interaction in the vicinity of half and quarter fillings.

Keywords: VCA, Mott metal-insulator transition, phase separation, first order phase transition, iridates, cuprates.

1 INTRODUCTION

Electron correlations found in several transition metal oxides and cuprates give rise to a broad range of different phenomena, leading to complex phase diagrams, phase separation (PS) instabilities and spatial inhomogeneities with nanoscale spatial variations of electron and spin densities [1-4]. The nanoscale phase separation effect is fundamental for understanding generic phases common for small and large thermodynamic systems. Spontaneous segregation of electron charge and spin density potentially plays an important role in defining electron charge pairing and ferromagnetism. The level crossings found in the two-dimensional (square) lattices generated by 8- and 10-site Betts unit cells [5] further point to the existence of quantum critical points for phase separation instabilities in large size systems. In this report, we further study the local mechanism of electronic phase separation, spin-orbit (SO) couping and geometric effects using quantum cluster calculations (QCCs) and the variational cluster approximation (VCA) in the two-dimensional (2d) Hubbard lattice in the absence of long-range order. The Hubbard model in square clusters and 2d lattices exhibit a metal-insulator transition at finite on-site Coulomb interactions U. In general, this transition at a finite U value might be an intrinsic property of the Mott metal-insulator transition in the Hubbard lattice away from half filling. There are several known striking qualitative effects of SO and magnetic field on electron correlation [6]. Below we explore the problem of PS instabilities in electron and spin densities by studying these effects near half and quarter fillings using different band topologies.

2 MODEL

We use the one-band Hubbard Hamiltonian $\hat{H}$ in a transverse magnetic field for repulsive (U>0) and attractive (U<0) electrons

$$\hat{H} = -\sum_{\langle i,j\rangle\sigma} te^{i\phi}\left(c^{+}_{i\sigma}c_{j\sigma} + h.c\right) + U\sum_{r} n_{i\uparrow}n_{i\downarrow} + \hat{V}_{so} \quad (1)$$

with magnetic field and spin-orbit coupling

$$\hat{V}_{so} = V_{so}\sum_{l}\left[\hat{c}^{+}_{l+x,\downarrow}\hat{c}_{l,\uparrow} - \hat{c}^{+}_{l+x,\uparrow}\hat{c}_{l,\downarrow} + i\left(\hat{c}^{+}_{l+y,\downarrow}\hat{c}_{l,\uparrow} + \hat{c}^{+}_{l+y,\uparrow}\hat{c}_{l,\downarrow}\right)\right] + h.c.$$

where the parameter ϕ in the transverse magnetic field is given in units of quantum phase ϕ_0=hc/e and transfer coupling parameter t *is* set to 1.

2.1 Band structure calculations (U=0)

Using non-interacting electron system with U=0 one can perform exact band structure calculations modeled with SO and magnetic field in assembled nano-ribbons (arrays of clusters) in (graphene) honeycomb and two leg square structures for understanding pyrochlore R_2Ir_2O and honeycomb Na_2IrO_3, Li_2IrO iridates and topological insulators, associated with numerous interfaces and heterostructures. Fig. 1 shows a spectrum of the four leg infinite 1d honeycomb ribbon (armchair) cuts out from the infinite 2d graphene sheet as a function of quantized flux at a given SO coupling.

3. PHASE SEPARATION

3.1 Quantum cluster calculations (U≠0)

The finite-size clusters may be one of the few solid grounds available to solve this challenging problem at

finite U by defining canonical and the grand canonical local gaps in the absence of true long-range order. Exact solutions in small cluster "molecules", i.e., the building blocks, or prototypes, of solids provide insight into the complexity of electron behavior in nanoparticles and respective bulk nanomaterials. A new guiding principle for the search of novel materials with electron instability is the proximity to the level crossing for spontaneous transitions attributed to intrinsic spatial inhomogeneities. The inhomogeneous concentrated system in equilibrium can be approximated as a quantum gas of decoupled quantum gas of clusters, which do not interact directly but exchange electrons through a thermal reservoir by allowing the energy and electron number to fluctuate. Below we use QCCs to model spin–orbit effects leading to distinct phases of matter.

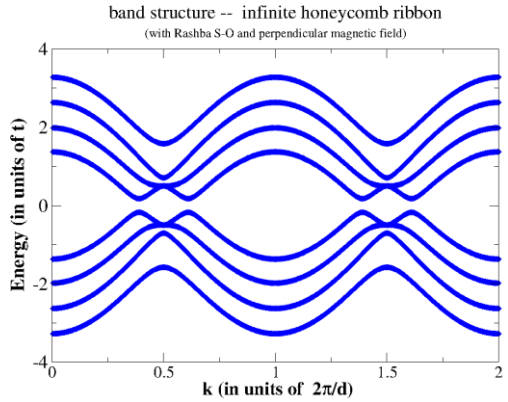

Fig. 1 The spectrum of the infinite (one-dimensional) four leg honeycomb ribbon structure inserted in the transverse magnetic field with the magnetic flux ϕ and SO coupling V_{so}=0.5t. The gap at the Fermi level (E=0 at half filling) arises due to the magnetic field which breaks time-reversal symmetry.

3.2 Level crossings

Once the exact eigenvalues and eigenstates are known, the statistical many-body problem can be constructed using exact thermodynamic expressions that can be analyzed without resorting to any approximations [7-9]. A collection of "clusters" can be treated at a fixed average number of electrons $\langle N\rangle$ and total spin $\langle S\rangle$ in a canonical ensemble. We define a charge gap as $\Delta^c=E(M+1,M';U:T)+E(M-1,M';U:T)-2E(M,M';U:T)$ using canonical energies $E(M, M'; U: T)$ with a given average number of electrons $N=M+M'$, U and temperature T determined by the number of up (M) and down (M') spins with the average spin, $S^z=\frac{1}{2}(M-M')$. The corresponding spin gap is defined as $\Delta^s = \frac{1}{2}[E(M+1, M'-1; U: T) + E(M-1, M'+1; U: T)-2E(M, M'; U: T)]$. As temperature approaches zero, the possible sign change in canonical gaps signifies the existence of level crossings related to first order (dramatic) changes away from half (or quarter) filling . The nodes of the charge gap, at which charge gap disappears, define the critical U points for the energy level crossings. The negative $\Delta^{c,\,s}$ gap regions display corresponding spontaneous PS instabilities.

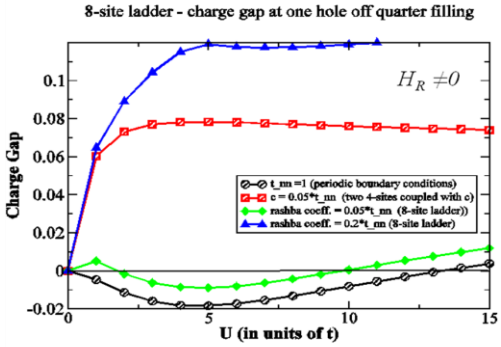

Fig. 2 Charge canonical gaps versus U at T = 0 for the 2×4 clusters with various couplings c between square clusters at one hole of quarter filling, $\langle N\rangle$=4. The weak SO favors the Mott metal-insulator transition away from quarter filling.. The negative gap regions correspond to an effective electron-electron attraction.

The spin–orbit interaction also has quantitative and qualitative effects on the correlation-driven Mott insulator transition. Fig. 2 shows the detrimental effects the of spin orbit term on the negative charge gap. The increase seen in the gap with $V_{so}\neq 0$ is similar to the effect of weakening the coupling between square clusters shown in Fig. 1. As expected, we do see a shift in the crossing point of U (from negative to positive gap) which provides stability for an insulating phase arising from Rashba SO coupling.

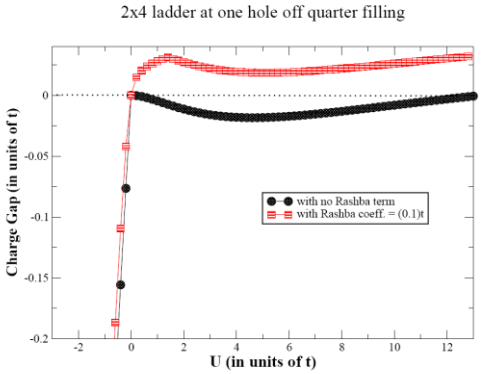

Fig. 3 Charge gap in 2x4 clusters with and without Rashba SO term as a function of U at T = 0 and one hole off quarter filling. In contrast to the U>0 region the changes in the charge gap at U<0 are insignificant.

3.3 Negative *U* Hubbard model

The phase separation with negative charge gap can be modeled in negative U Hubbard clusters. Fig. 3

displays the differences in behavior of attractive and repulsive Hubbard models with regard to the SO coupling. Notice, there is a significant shift in the crossing point in the vicinity of U=12.

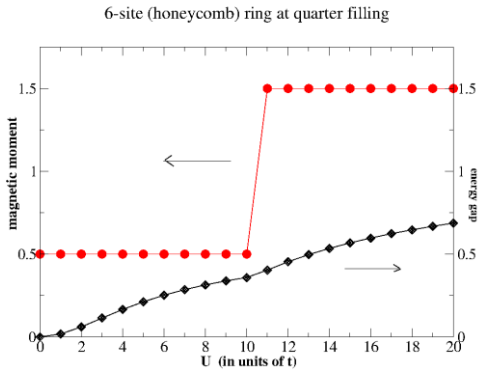

Fig. 4. Charge gap Δ^c of honeycomb cluster at quarter filling as a function of U and T = 0. The (positive) charge gap opens at infinitesimal U and increases monotonically. The negative spin gap corresponds to a phase separation instability in the spin density sector which manifests the transition near U=10 from an unsaturated magnetic moment S=1/2 into a fully saturated ferromagnetic with S_{max}=3/2.

3.4 Saturated ferromagnetism

We examine the effect of spontaneous phase separation in the spin density at quarter filling driven by U. Nagaoka-type intrinsic ferromagnetism is illustrated in Fig. 4 in a 6-site ring which shows a stable Mott insulating gap coexisting with the negative spin gap. This picture closely resembles Nagaoka ferromagnetism in 2d systems [10]. This result points to the possible existence of insulating ferromagnetism in graphene-like systems near optimal doping (quarter filling).

3.5 Cluster geometry

We study also the effect of cluster geometry on the mechanism of phase separation. In Fig. 5, a positive gap opens at infinitesimal U and increases monotonically avoiding level crossings, i.e., there is no sign of a PS instability. In inhomogeneous concentrated systems, this description in thermodynamic equilibrium becomes quite accurate for suitable values of parameters since the lattice can be broken up into periodic arrays of weakly coupled clusters. In the VCA, the cluster-cluster interaction is usually added through the coupling between the unit cells comparable to the energy transfer scale t within the cluster. Below we compare the geometry dependence in bipartite square and honeycomb lattices using the disconnected square and honeycomb clusters (that were solved exactly) as a reference system in VCA.

4. VCA CALCULATIONS

Here we use the VCA [9] to solve the problem of PS in the Hubbard model on a large-size lattice by diagonalization in real space. Below, we investigate possible phase separation in both square and honeycomb lattices from half-filling to optimal doping using VCA.

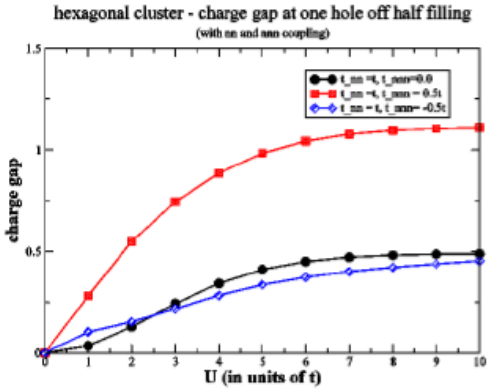

Fig. 5 The electron charge gap in honeycomb 6-ste clusters with $\langle N\rangle$=5 electrons versus U with next nearest coupling at T=0. In contrast to square geometry, the charge gap evolves smoothly without level crossings as a function of U.

This method is quite accurate for calculation of short-range correlations. The grand potential Ω of the original system can be written as a functional of the self-energy Σ provided the system is not at a critical point associated with a phase transition [11]

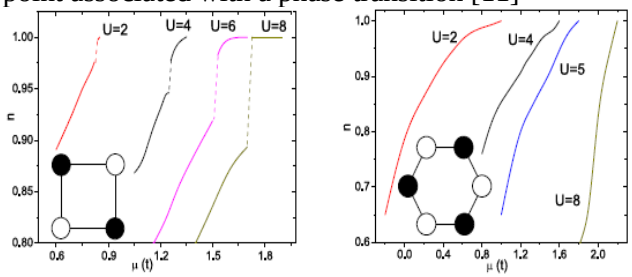

Fig. 6 The electron filling factor n versus μ for the Hubbard model at different $U>U_C$ values. (left) The discontinuities at distinct n values in the square lattice with different n at two edges of the step-like discontinuous transition have the same μ value. The plots for the honeycomb lattice are smooth, without discontinuities, i.e., PS is absent in this lattice. The reference systems used in the VCA calculation are shown in the inset of corresponding plots.

4.1 Mott transition at half filling

In two dimensions, our VCA calculations for the geometries provide strong support for a smooth second order metal-insulator transition at finite U at half filling. An energy gap is opened around the Fermi level at finite critical U in the one-particle excitation spectra for both (square and honeycomb) lattices.

4.2 Away from half filling

Phase separation, caused by electron instabilities under hole doping, leads to the coexistence of inhomogeneous, hole-rich and hole-poor regions. This phenomenon closely resembles phase separation instabilities observed in first order phase transitions. The coexisting states with different electron densities n share the same chemical potential μ. The phase separation scenario is illustrated in Fig. 6 (left). We find strong evidence of phase separation for the square lattice in the underdoped region, however, there is no sign of phase separation in the honeycomb lattice.

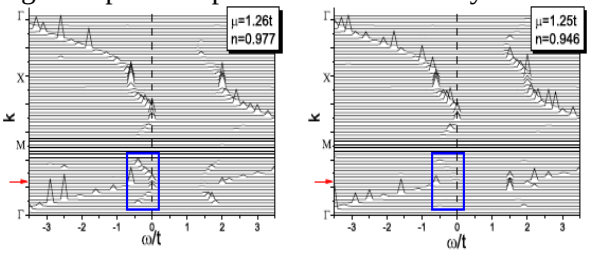

Fig. 7 One-particle excitation spectral functions for the Hubbard model at U=4 for the square lattice right before and after phase separation are shown at (left) an insulator with μ=1.26 (n=0.977) (right) a metal with μ=1.25 (n=0.947). The dotted line at ω=0 denotes the Fermi level. At the higher electron density (n=0.977), a part of spectra in (left), which is enclosed in the blue square, shows up around the Q point (marked by red arrow) at the Fermi level, but it vanishes in (right) at the lower density n=0.947 (almost no peaks in the blue square).

5. SPECTRAL FUNCTION

We have also extracted the spectral function for the two densities right before and after the electronic phase separation in the square lattice. The single particle excitation spectrum at U=4 of the square lattice is shown in Fig. 7. By comparing the spectral functions at the two densities, one can find that a set of narrow spectra around the Fermi surface (FS) at Q=($\pm\pi$/2a, $\pm\pi$/2a) point (see the red arrow in Fig. 7 between the Γ and M points) which disappears when the density drops from 0.977 to 0.946. This indicates that the states near Q become unstable as phase separation occurs. The scattering transfer momenta at Q reside on the boundary of the folded first Brillouin zone (FBZ) due to the period doubling of the lattice parameter, since the primitive unit cell of AF state contains two sites. The FS coincides with the borders of the AF FBZ with complete "nesting" after a translation by the Q vector of AF local ordering.

6, CONCLUSIONS

We have studied possible phase separations due to electronic correlations in bipartite square and honeycomb structures. The VCA calculations in square clusters provide strong support for our previous findings about the role of the local lattice structure at a PS instability, *i.e*., the lattice geometry plays a crucial role in the reconstruction of the FBZ. Upon increasing n towards half filling, there is a critical concentration n_c for a first-order transition between a metal and a Mott insulator at nonzero doping. The scenario obtained for phase separation is consistent with the Mott insulator behavior where a transition to the correlated insulator state occurs through a first-order phase transition induced by tuning correlation strength, temperature or doping [11]. The exact quantum cluster calculations in various building block structures demonstrate strong many body effects tied with Rashba SO and magnetic fields that can be related to pyrochlore and honeycomb iridate heterostructures. The results also provide insights into the microscopic electronic structure of bandgap-engineered graphene-type nanoribbon heterojunctions.

1 ACKNOWLEDGMENTS

The authors acknowledge the computing facilities provided by the Center for Integrated Nanotechnologies, a U.S. Department of Energy, Office of Basic Energy Sciences user facility at Los Alamos National Laboratory (Contract DE-AC52-06NA25396). The work was performed also, in part, at the Center for Functional Nanomaterials, Brookhaven National Laboratory supported by the U.S. Department of Energy, Office of Basic Energy Sciences, under Contract No.DE-AC02-98CH10886.

REFERENCES

[1] Tranquada JM, Sternlieb BJ, Axe JD, Nakamura Y, Uchida S375, 561 (1995)
[2] Hoffman JE, Hudson EW, Lang KM, Madhavan V, Eisaki H, Uchida S, Davis JC, Science 295, 466 (2002)
[3] Visscher PB, Phys. Rev. B 10:943 (1974)
[4] Emery VJ, Kivelson SA, Lin HQ, Phys. Rev. Lett. 64, 475 (1990)
[5] Kocharian AN, Kun Fang, Fernando GW, JMMM 324 3427 (2012)
[6] W-Krempa W, Chen G, Kim YB, and Balents L, Ann. Rev. Cond. Matt. Phys. 5, 57 (2014)
[7] Kocharian AN, Fernando GW, Palandage K, Davenport JW, Phys. Rev. B74, 024511 (2006)
[8] Fernando GW, Palandage K, Kocharian AN, Davenport JW Phys. Rev. B80, 014525 (2009)
[9] Kocharian AN, Fernando GW, Palandage K, Davenport JW Phys. Rev. B78, 075431 (2008).
[10] Nagaoka Y., Phys. Rev. 147, 392 (1966).
[11] Aichhorn M, Arrigoni E, Potthoff M, Hanke W, Phys. Rev. B 74, 235117 (2006)
[12] G. Sordi, K. Haule, A.-M. S. Tremblay, Phys. Rev. B84, 075161 (2011)